Structural Engineering and Mechanics, *Vol. 75, No. 3 (2020) 295-309*
DOI: https://doi.org/10.12989/sem.2020.75.3.295

Optimization of the seismic performance of masonry infilled R/C buildings at the stage of design using artificial neural networks

Konstantinos G. Kostinakis*[1] and Konstantinos E. Morfidis[2a]

[1]Department of Civil Engineering, Aristotle University of Thessaloniki, 54124, Thessaloniki, Greece
[2]Institute of Engineering Seismology and Earthquake Engineering (ITSAK-EPPO), 55535, Thessaloniki, Greece

(Received April 18, 2019, Revised February 17, 2020, Accepted February 21, 2020)

Abstract. The construction of Reinforced Concrete (R/C) buildings with unreinforced masonry infills is part of the traditional building practice in many countries with regions of high seismicity throughout the world. When these buildings are subjected to seismic motions the presence of masonry infills and especially their configuration can highly influence the seismic damage state. The capability to avoid configurations of masonry infills prone to seismic damage at the stage of initial architectural concept would be significantly definitive in the context of Performance-Based Earthquake Engineering. Along these lines, the present paper investigates the potential of instant prediction of the damage response of R/C buildings with various configurations of masonry infills utilizing Artificial Neural Networks (ANNs). To this end, Multilayer Feedforward Perceptron networks are utilized and the problem is formulated as pattern recognition problem. The ANNs' training data-set is created by means of Nonlinear Time History Analyses of 5 R/C buildings with a large number of different masonry infills' distributions, which are subjected to 65 earthquakes. The structural damage is expressed in terms of the Maximum Interstorey Drift Ratio. The most significant conclusion which is extracted is that the ANNs can reliably estimate the influence of masonry infills' configurations on the seismic damage level of R/C buildings incorporating their optimum design.

Keywords: reinforced concrete buildings; masonry infills; seismic damage; artificial neural networks; pattern recognition

1. Introduction

The seismic response of Reinforced Concrete (R/C) buildings is a polyparametric problem which is affected by the structural parameters of buildings, the characteristics of earthquakes that are expected to hit them (seismic parameters) and the local site effects (soil parameters). The degree at which these parameters affect the seismic response of R/C buildings has been investigated and is still under investigation (Pauley and Priestley 1992, Kappos and Penelis 1997), since the uncertainties associated with them are important. Among the abovementioned three types of parameters that influence the buildings' seismic response, and consequently, their seismic vulnerability, the only one that can be optimized at the stage of their design is the structural parameters. For example, at the stage of the building's design, the civil engineer can form the load bearing system in such a way (e.g. using R/C walls, conducting capacity design of joints, forming structures that are regular in elevation and in plan, minimizing the structural eccentricities etc) that effects with negative influence on its seismic response are prevented. Note that these choices that minimize the negative effects which can be induced by the structural parameters have been adopted by all the current seismic code provisions (e.g. see EN1998-1 2003, IBC-2018, ATC-63 2008).

*Corresponding author, Ph.D., Assistant Professor
E-mail: kkostina@civil.auth.gr
[a] Ph.D., Assistant Researcher
E-mail: konmorf@gmail.com

The construction of R/C buildings with unreinforced masonry infills is part of the traditional building practice in many countries with regions of high seismicity throughout the world. The infill panels are usually considered to be the best method to fulfill functional and architectural or aesthetic needs. However, because of the complexity of the problem and the uncertainties associated with the proper modeling of the masonry infill panels, their interactions with the R/C structural elements and, consequently their influence on the seismic response of buildings are often neglected. Thus, the infill walls are usually considered as non-structural elements and are not taken into account in the computational models. This assumption has been adopted by the majority of the current seismic code provisions. However, the observation of post-earthquake damages on R/C structures has led to the conclusion that the presence of masonry infills may significantly alter the seismic performance of buildings (e.g. EERI 1999, Ricci *et al*. 2010). More specifically, experimental and numerical researches have shown that a uniform distribution of masonry infill walls can lead to the increase of lateral stiffness and robustness (e.g. Bettero and Brokken 1983, Ricci *et al*. 2011, Mondal and Tesfamariam 2014), whereas, if the masonry infills are unevenly distributed, negative effects may be induced, such as the soft storey mechanism. For the above-mentioned reasons, the influence of the masonry infills on the nonlinear response of R/C buildings can be crucial, as it has been shown by numerous studies. For example, Manfredi *et al*. (2012) investigated the influence of infills on the seismic behavior of a case-study

http://www.techno-press.com/journals/sem&subpage=7
ISSN: 1225-4568 (Print), 1598-6217 (Online)

existing gravity load designed R/C building. The analyses revealed that the presence of regularly distributed infills provides a beneficial increase in stiffness and strength, whereas when there is an irregular distribution of masonry infills detrimental effects due to the sudden loss of strength are present. In a similar research, Ricci *et al*. (2013) conducted a numerical investigation on the influence of infills on the seismic behavior of four different case study buildings. Fiore *et al*. (2012) conducted nonlinear static analyses of two R/C existing buildings located in a high seismic hazard area. Numerical analyses were performed by using spatial models, both for the bare and the infilled frames. The analyses showed that the presence of the infill panels can influence the global collapse mechanisms under seismic actions depending on the building's characteristics. Another investigation was carried out by Mondal and Tesfamariam (2014), who conducted nonlinear static analyses of a six-storey R/C frames in order to quantify the effects of vertical irregularity and thickness of masonry infills on the robustness of structures. They found that these infills' properties have significant influence on the response of the R/C frames. More recently, Kostinakis *et al*. (2018) examined the seismic behavior of planar multistorey R/C buildings with various masonry infills' distributions in the context of Incremental Dynamic analysis. The results of the study demonstrated that the presence of the masonry infills cannot be ignored, since they strongly influence the inelastic dynamic response of buildings.

The extensive investigation of the masonry infills' influence (positive or negative), a small part of which has been presented above, proves the high degree of uncertainties that they introduce in the seismic response. This fact has led the current seismic codes, e.g. EN1998-1 (2003) to import provisions, the application of which depends on the positive or negative role of the infills on the buildings' seismic response.

Moreover, the seismic codes state that the distribution of the masonry infills should not induce major plan eccentricities or increase the eccentricities that are due to the configuration of the load bearing system's elements. Thus, it is evident that the infills' distribution consists one of the critical parameters that should be taken into account during the initial stage of R/C building's design. However, a preliminary assessment of the degree of eccentricity that is induced by the masonry infills at the design stage is not adequate, since it is usually estimated under the assumption that the buildings' structural (and non-structural) members remain elastic during the earthquake. Yet, it is well known that during a strong seismic motion (minor or major) damages are possible to be caused on the infills, thus differentiating the eccentricity that has been estimated using the assumption of the elastic behavior. Therefore, it would be more reliable and realistic to estimate the influence of the infills' distribution that is proposed at the stage of the design on the seismic vulnerability of R/C buildings with the aid of Nonlinear Time History Analyses (NTHA). Nevertheless, although the computational power of the modern hardware and software make these analyses feasible, the conduction of them for a limited number of certain seismic motions, even though they may be chosen using appropriate methodologies, is likely to lead to non-reliable results. The reason is that it is always possible to find an earthquake with characteristics completely different from those of the motions for which the analyses were conducted.

In order to deal with the problem of the estimation of the infills' distribution on R/C buildings' seismic vulnerability at the stage of their design an alternative approach based on the utilization of Artificial Neural Networks (ANNs) is introduced in the present study. The ANNs are complex computational structures that are based on the general rules of the biological brain (see e.g. Fausett 1994, Haykin 2009), which is capable of recalling the knowledge that has acquired during its training in order to deal with known type of problems with unknown characteristics (that appear for the first time). Moreover, the capability of ANNs to achieve realistic estimation of solution of polyparametric problems at a very short time due to the significant increase of the computational power of the hardware and the software in the last years has led to their use for the solution of a large number of problems in the fields of medicine, telecommunications, function of electric or electronic devices, industrial equipment etc. Besides, numerous are also the applications of the ANNs at the scientific area of the civil engineering (see e.g. Adeli 2001, Jegadesh and Jayalekshmi 2015). Focusing on the field of the seismic induced damage identification through the utilization of ANNs, many research works have been published (see e.g. Latour *et al*. 2009, Vafaei *et al*. 2011, 2013 and 2014, Akbas *et al*. 2011, Lagaros and Papadrakakis 2012, Morfidis and Kostinakis 2017, 2018, 2019).

The objective of the present paper is to examine the ability of Multilayer Feedforward Perceptron (MFP) networks with one or two hidden layers to adequately predict the seismic damage level of R/C buildings with various distributions of masonry infills. To accomplish this purpose an extensive parametric study was carried out. More specifically, in order to create the required training data-set for the MFP networks, five 5-storey R/C buildings with symmetric plan view and different structural systems (with or without r/c shear walls in one or two perpendicular axes) were studied. For each building a large number of different masonry infills' distributions was considered, and individual training data sets were created. Thus, five training data-sets for each one of the studied buildings were developed. The buildings were analyzed by means of NTHA for 65 bidirectional strong motions and four different incident angles (θ=0°, 90°, 180° and 270°) which influence strongly the results (e.g. Rigato and Medina 2007, Nguyen and Kim 2013, Kostinakis *et al*. 2013, Fontara *et al*. 2015, Kostinakis *et al*. 2015, Kostinakis *et al*. 2018). For the evaluation of seismic damage, the Maximum Interstorey Drift Ratio (MIDR) was utilized (Gunturi and Shah 1992, Naeim 2001). The problem was formulated and solved as a Pattern Recognition (PR) problem (e.g. Ripley 1996, Theodoridis and Koutroumbas 2008, Asht and Dass 2012). This choice was made because the target is mainly the estimation (at the stage of the initial design of buildings) of the level of seismic damage which is expected due to the various distributions of masonry infills and not the strict calculation of the expected value of the seismic damage index (MIDR). Moreover, as it was proved (e.g. Morfidis and Kostinakis 2017, 2018) the solution of the PR problems using ANNs leads to very reliable results as regards the classification of R/C buildings in pre-defined (three or five) damage classes. Finally, it must be stressed that at the stage of the initial concept of a building's design where the vast majority of its features are under investigation, the utilization of a soft computing technique is a sufficient approach which is also not time consuming. Thus, every desirable distribution of masonry infills can be rapidly evaluated without the need of utilization of NTHA.

2. Procedure for the generation of the training data set of networks

In this section the procedure adopted in order to generate the data set for the ANNs' training will be presented. This procedure consists of certain steps, such as the selection, the modeling and the design of the R/C buildings that were used for the present investigation and the selection of the seismic motions for which these buildings were analyzed utilizing NTHA. By the post processing of the analyses' results the values of the seismic damage index MIDR were computed. These values are the main elements of the data set's target vectors. Comprehensive description of the procedure followed in order to generate training data sets for problems concerning the prediction of R/C buildings' seismic vulnerability can be found in Morfidis and Kostinakis (2018).

2.1 The Investigated Buildings – Selection, Modeling Assumptions and Design

For the purposes of the present investigation, five 5-storey double-symmetric in plan R/C buildings, with data supplied in Appendix A were studied. All buildings have structural system that consists of members in two perpendicular directions (axes x and y, Fig. A.1) and are regular in elevation and in plan according to the criteria set by EN1998-1. They differ in the ratios of base shear that are received by R/C walls (if exist) along two perpendicular axes (axes x: n_{vx} and y: n_{vy}). In Table A.1 of Appendix A all the common design data of the examined buildings are presented. For the buildings' modelling all basic recommendations of EN1998-1, such as the diaphragmatic behavior of the slabs, the rigid zones in the joint regions of beams/columns and beams/walls and the values of flexural and shear stiffness corresponding to cracked R/C elements were taken into consideration. All buildings were considered to be fully fixed to the ground. Using the data given in Table A.1, the upper limit values of the behavior factor q according to EN1998-1 were determined (Fig. A.1). All buildings were designed for static vertical loads as well as for earthquake loads (taking into consideration the accidental torsion effects) using the modal response spectrum analysis, as defined in EN1998-1. The R/C structural members were designed following the provisions of EN1992-1-1 (1991) and EN1998-1 (2003).

For the modeling of the buildings' nonlinear behavior lumped plasticity models (plastic hinges) at the column and beam ends, as well as at the base of the walls, were used. The material inelasticity of the structural members was modeled by means of the Modified Takeda hysteresis rule (Otani 1974). It must be stressed that the effects of axial load-biaxial bending moments (P-M_1-M_2) interaction at columns and walls hinges were taken into consideration by means of the P-M_1-M_2 interaction diagram which is implemented in the software used to conduct the analyses (Carr 2004). The yield moments of all R/C elements as well as the parameters needed to determine the P-M_1-M_2 interaction diagram of the vertical R/C elements' cross sections were determined using the XTRACT software (2006).

2.2 Masonry Infills - Modeling assumptions and description parameters

In order to capture the effects caused by the arbitrary placement of masonry infills, a large number of different distributions of them for each one of the five selected buildings were adopted. Note that the scope of the present research is to study the effects of in-plan irregularities on the seismic response of R/C buildings. Thus, the same configuration of the masonry infills was used for all the five storeys of all buildings in order to avoid effects caused by the irregular placement of the infills along their height. Furhermore, it must be noticed that only infill distributions with masonries present in all the spans of the frames were considered. Every infilled building can be characterized by the use of several structural parameters. For the needs of the present investigation, the following parameters were adopted:

(a) The eccentricities ($e_{mas,x}$ and $e_{mas,y}$) of storeys which are caused by the location of masonries. These eccentricities are equal to the distance between the mass centre of the storeys of the infilled building and the mass centre of the storeys of the corresponding bare building (which coincides with the geometric mass centre of them) along the axes x and y (see Fig. 1). The eccentricity of storey's mass is considered as a parameter that can adequately capture the degree of irregularity caused by the non-uniform distribution of the infills in plan, since, in case of double-symmetric buildings, it only depends on their specific configuration. Note that the modern seismic codes (e.g. EN1998-1 2003, §4.2.3.2) use parameters based on calculation of storeys' eccentricities in order to estimate the in-plan irregularity of buildings.

(b) Ratios of the masonry infills along the structural axes x and y, which are given by Eq.(1).

$$n_{mas,x} = \frac{W_{mas,x}}{maxW_{mas,x}} \qquad n_{mas,y} = \frac{W_{mas,y}}{maxW_{mas,y}} \tag{1}$$

where $W_{mas,x}$ is the weight of the masonry infills along the axis x, $maxW_{mas,x}$ is the maximum weight of the infills along the axis x (i.e. the masonry infills' weight in the case in which they are present at all spans parallel to the axis x), $W_{mas,y}$ is the weight of the masonry infills along the axis y, $maxW_{mas,y}$ is the maximum weight of the masonry infills along the axis y (i.e. the masonry infills' weight in the case in which they are present at all spans parallel to the axis y).

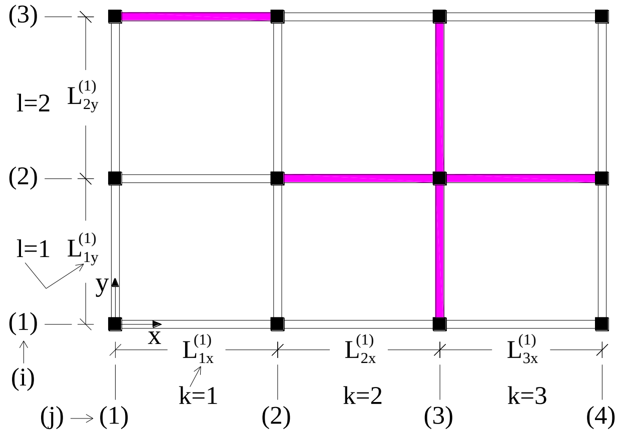

$$\max W_{mas,x} = h_{st} \cdot \sum_{i=1}^{3}\sum_{k=1}^{3}\left[g^{(i)}_{kx} \cdot L^{(i)}_{kx}\right]$$

$$\max W_{mas,y} = h_{st} \cdot \sum_{j=1}^{4}\sum_{l=1}^{2}\left[g^{(j)}_{ly} \cdot L^{(j)}_{ly}\right]$$

$$W_{mas,x} = h_{st} \cdot \left[g^{(3)}_{1x} \cdot L^{(3)}_{1x} + g^{(2)}_{2x} \cdot L^{(2)}_{2x} + g^{(2)}_{3x} \cdot L^{(2)}_{3x}\right]$$

$$W_{mas,y} = h_{st} \cdot \left[g^{(3)}_{1y} \cdot L^{(3)}_{1y} + g^{(3)}_{2y} \cdot L^{(3)}_{2y}\right]$$

h_{st} =storey's height (m)

g =the weight of masonry infillper unit of area (kN/m^2)

Fig. 1 Procedure of calculation of the selected input structural parameters

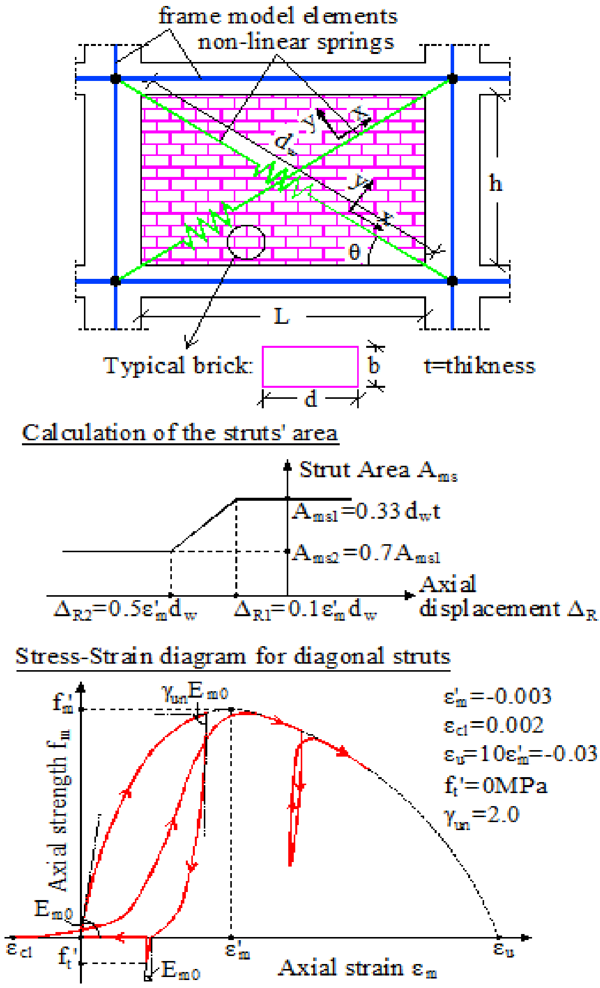

$$f'_m = f'_{m\theta} = \min\left\{f'_{m\theta1}, f'_{m\theta2}\right\}$$

$$f'_{m\theta1} = \frac{\tau_0^*}{\sin\theta\left(\cos\theta - \mu^*\sin\theta\right)}$$

$$f'_{m\theta2} = \frac{f'_{fb}}{\sin\theta\left(C_s\cos\theta - 0.27\sin\theta\right)},\ f'_{fb} = 1.05\text{MPa}$$

$$\tau_0^* = \frac{\tau_0}{1+\mu C_u\left(b/d\right)},\ \mu^* = \frac{\mu}{1+\mu C_u\left(b/d\right)}$$

$$\mu = 0.7,\ \tau_0 = 0.5\text{MPa},\ C_u = 1.5$$

Fig. 2 Modeling of the masonry infill panels' seismic response using the method of diagonal struts

The explanation of the above described terms is better illustrated with the aim of the example of Fig. 1. It must be noticed that the different distributions of the masonry infills were selected arbitrarily, trying to cover a wide range of all possible values of the above structural parameters. Thus, 1017 different infills' distributions were considered in total for the five buildings (293 for the SFxy, 149 for the SWxy, 141 for the SWxFy, 293 for the SFExy and 141 for the SFExFy).

Concerning the modeling of each masonry infill panel, in the present study, the single equivalent diagonal strut model was adopted. This model does not account for the local failure of the node, but it only participates in the global collapse mechanism of the building, which is the main objective of the present research. More specifically, each infill panel was modeled as a single equivalent diagonal strut with stress-strain diagram based on the model proposed by Crisafulli (1997), as shown in Fig.2. In the same figure, all the basic parameters used to define the properties of the diagonal struts are presented. It must be noticed that in the present work the values of these parameters were determined based on the code provisions given in EN1996-1-1 (2005).

2.3 The selected ground motions for the NTHA

A suite of 65 pairs of horizontal bidirectional earthquake excitations obtained from the PEER (2003) and the European strong motion database (2003) was used as input ground motion for the analyses which were performed in order to generate the networks' training data set. The seismic excitations, which have been chosen from worldwide well-known sites with strong seismic activity, are recorded on Soil Type C according to EN1998-1 and have magnitudes (M_s) between 5.5 and 7.8. The ground motion set employed was intended to cover a variety of conditions regarding tectonic environment, modified Mercalli intensity and closest distance to fault rapture, thus representing a wide range of intensities and frequency content. Another important aspect considering the selection of the seismic excitations is that they provide a wide spectrum of structural damage, from negligible to severe, to the buildings investigated in the present study. Moreover, note that the unscaled accelerograms have been used for the nonlinear dynamic analyses, because scaling of the earthquake records would give a falsified value of the interdependency between the seismic parameters and the structural damage.

2.4 Description of the training data set

As it is well-known, ANNs' training data sets consist of a number of input vectors and the corresponding target vectors (see e.g. Fausett 1994, Haykin 2009). As regards the input vectors, these are composed by the parameters which are selected in order to describe the problem. In the present study, where the problem regards the prediction of the differentiation of the R/C buildings' seismic vulnerability due to the masonry infills distribution, the chosen parameters should be structural as well as seismic ones. More specifically, the structural parameters should concern both the configuration of R/C buildings' load bearing system and the distribution of their masonry infills. Regarding the parameters that describe the configuration of the load bearing system, in general, in the approximate methods of estimation of the R/C buildings' seismic vulnerability, parameters that describe the load bearing system of buildings in a macroscopic way can be adopted (e.g. ATC-13 1985, Anagnos *et al*. 1995, Kappos *et al*. 2006, Morfidis and Kostinakis 2018). Such parameters are e.g. the buildings' height, the existence or not of R/C walls and the ratio of the seismic base shear that they receive if they exist, as well as the storeys'eccentricity (i.e. the distance between their mass centre and their stiffness centre). In the present investigation it was decided to generate 5 different training data sets for the 5 different buildings' types that they were considered. As a consequence, the insertion of parameters that describe the configuration of the load bearing system in the input vectors is not necessary, since each one of the 5 different training data sets corresponds to a certain building type (each one of the training data sets consists of 10660 samples (SFxy), 10660 samples (SFExy), 9165 samples (SFExFy), 9165 samples (SWxFy) and 9685 samples (SWxy)). Thus, the only structural parameters that were inserted in the input vectors are those that describe the distribution of the masonry infills. These structural parameters were described in previous section (Eq.1 and Fig. 1). It must be stressed at this point that another one parameter which should be imported to input vectors is the stiffness of the infill walls which has a great influence on the calculated eccentricities. However, this parameter was not taken into consideration in the present investigation, not because it is not important but because the aim of the present paper is the presentation and the testing of the ability of ANNs to be used for the optimization of the seismic performance of infilled r/c buildings at the stage of design and not a parametric investigation of the impact of masonry characteristics on the seismic damage. Thus, the assumption that all masonry infills of all buildings which were used for the generation of the training data-sets have the same stiffness was made. For this reason, the stiffness of the infill walls is not necessary to be included in the input vectors. Nevertheless, it must be stressed that in case of the practical application of ANNs for the optimization of the seismic performance of infilled r/c buildings at the stage of design this parameter must be inserted to input vectors. This insertion, does not change the concept and the special characteristics of the proposed method as it is presented in the current paper.

Table 1 The selected seismic parameters and the ranges of their values corresponding to the 65 earthquakes

Ground Motion Parameter	Min Value	Max Value
Peak Ground Acceleration - PGA	0.004g	0.822g
Peak Ground Velocity -PGV	0.86 cm/sec	99.35 cm/sec
Peak Ground Displacement - PGD	0.36 cm	60.19 cm
Arias IntensityI_a	≈0.0 m/sec	5.592 m/sec
Specific Energy Density - SED	1.24cm^2/sec	16762.8cm^2/sec
Cumulative Absolute Velocity-CAV	14.67cm/sec	2684.1cm/sec
Acceleration Spectrum Intensity-ASI	0.003 g·sec	0.633 g·sec
Housner Intensity - HI	3.94 cm	317.6 cm
Effective Peak Acceleration - EPA	0.003g	0.63g
V_{max}/A_{max} (PGV/PGA)	0. 036 sec	0.336 sec
PredominantPeriod - PP	0.077 sec	1.26 sec
Uniform Duration - UD	≈0.0 sec	17.68 sec
Bracketed Duration - BD	≈0.0 sec	61.87 sec
Significant Duration - SD	1.74 sec	50.98 sec

As regards the seismic parameters which are used to describe the seismic excitations and their impact on R/C buildings, there are many definitions which are resulted from the analysis of accelerograms records (see e.g. Kramer 1996). For the investigation conducted in the present study, the 14 seismic parameters which are illustrated in Table 1 have been chosen. It must be noted that the big number of the ground motion parameters was used in order to model the seismic influence on the damage response as precisely as possible. It is also well-known that in case of multiparametric problems a sensitivity analysis in order to determine the most influential parameters is advisable. The conduction of sensitivity analysis for the detection of the most influential ground motion parameters is out of the scope of the present paper (despite the fact that it is possible to lead to more precise results), which is concentrated on the presentation of the procedure for the optimization of infilled r/c buildings' seismic performance at the stage of their design using ANNs. However, it must be stressed that a sensitivity analysis which was conducted by Morfidis and Kostinakis (2017) led to the conclusion that adequate modeling of seismic excitations in the framework of the damage prediction of r/c buildings using ANNs can be achieved using at least 6 seismic ground motion parameters, while optimum modeling is achieved when the 14 seismic ground motion parameters which are illustrated in Table 1 are used.

Thus, the input vectors consist of 18 (4 structural and 14 seismic) parameters. Namely, they are vectors with dimension 18x1 and have the general form which is given by the Eq. (2):

$$
\begin{aligned}
&\mathbf{x} = \left[\mathbf{x}_{seism} \mid \mathbf{x}_{struct}\right]^T \\
&\mathbf{x}_{seism} = \left[\mathrm{PGA} \mid \mathrm{PGV} \mid \mathrm{PGD} \mid \mathrm{I_a} \mid \mathrm{SED} \mid \mathrm{CAV} \mid \mathrm{ASI} \mid \right. \\
&\qquad \left. \mid \mathrm{HI} \mid \mathrm{EPA} \mid \mathrm{PGV/PGA} \mid \mathrm{PP} \mid \mathrm{UD} \mid \mathrm{BD} \mid \mathrm{SD}\right]^T \qquad (2) \\
&\mathbf{x}_{struct} = \left[n_{mas,x} \mid n_{mas,y} \mid e_{x,mas} \mid e_{y,mas}\right]^T
\end{aligned}
$$

Table 2 Relation between MIDR values and damage levels – 5 or 3 damage classes

MIDR (%)		*<0.25*	*0.25-0.5*	*0.5-1.0*	*1.0-1.5*	*>1.5*
Damage level (class)	1st approach	Null	Slight	Moderate	Heavy	Collapse
	2nd approach	Slight (No damages or repairable slight damages)		Moderate (Significant but repairable damages)	Heavy/Collapse (non-repairable damages)	

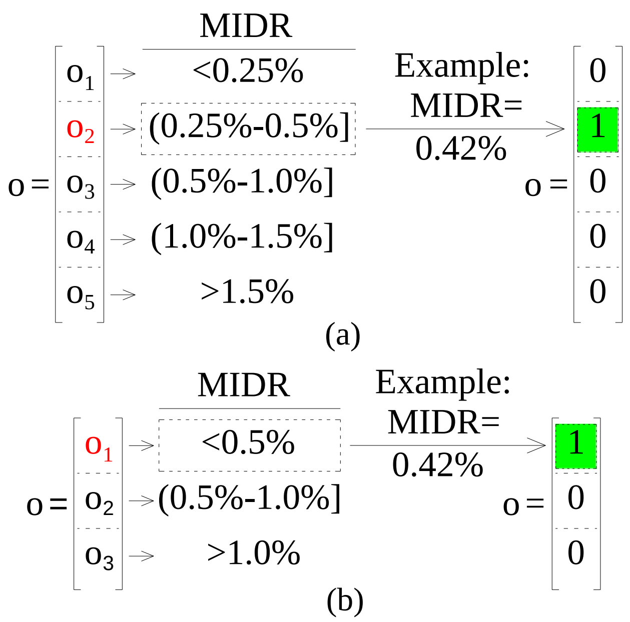

Fig. 3 Procedure of mapping between the output vectors o and the pre-defined damage levels in case of: (a) 5 damage levels, (b) 3 damage levels

Regarding the target vectors, it should be noticed that they must be formulated on the basis of the requirements of pattern recognition problems. The choice of formulation of the investigated problem in terms of pattern recognition (as mentioned in the introduction) was based on the fact that the main target is the estimation (at the stage of the initial design of buildings) of the level of seismic damage which is expected due to the various distributions of masonry infills and not the strict calculation of the expected value of the seismic damage index.

The formulation in terms of a pattern recognition problem requires the definition of classes into which the target vectors can be classified. These classes, in the context of the present investigation, should be defined as specific ranges of values that the damage index can attain. As mentioned in the introduction, the seismic damage index which was selected in the present study is the Maximum Interstorey Drift Ratio (MIDR). The procedure for the calculation of MIDR in the framework of NTHA can be found in Morfidis, K. and Kostinakis, K. (2017). For the relation between the values of MIDR and the R/C buildings' damage classes two approaches were adopted in the present study. According to the first one, the MIDR values were classified into 5 damage classes according to the Table 2 (see e.g. Masi *et al*. 2011).

According to the second approach, the number of the damage classes was reduced to 3 through the merge of the first two and the last two damage classes of the classification in 5 classes (Table 2). The aim of consideration of the second approach was to assess the ANNs' efficiency using a more slapstick description of the damage levels, which can be considered adequate in the case in which a rapid assessment of seismic damages of R/C buildings is required. Moreover, such a classification of damages is more compatible with the approach "Green" - "Yellow" - "Red" (Slight Damage – Moderate Damage – Heavy Damage), which has already been widely adopted for rapid estimation of the seismic damage level. After the definition of the damage classes and their relation with the MIDR values (Table 2), the mapping of these classes with certain configurations of the output vectors should be defined (Fig. 3). According to Figure 3 the dimensions of the output vectors are equal to the number of the damage levels, whereas their elements attain the value 1 when the value of MIDR lies within the range of the damage level values which they represent. Otherwise, they attain the value 0.

3. Parametric investigation for the optimum configuration of networks

In general, the parameters which are required for the configuration of the MFP networks are the following: (a) the number of the hidden layers; (b) the number of neurons in each hidden layer; (c) the activation functions of neurons; (d) the performance evaluation parameters; (e) the normalization functions of the input and output values and (f) the method for partitioning the data set in training, validation and testing subsets. In the present study, specific choices for some of the aforementioned parameters were made, while for some other more than one choice was made in order to detect the network which extracts the optimum predictions (optimum configured network). These choices are the following:

(a) Number of the hidden layers: Networks with a one and two hidden layers were selected.

(b) Number of neurons in hidden layers: The optimum number of neurons in hidden layers is not uniquely defined for all problems. Furthermore, there is no a direct method for its determination. Thus, the "trial and error" method is always adopted. In the context of the present study, an investigation for the determination of the optimum number of neurons in hidden layers was conducted. More specifically, networks with a number of neurons in hidden layers that ranges between 10 and 60 were configured. Then, the number of neurons in hidden layers that led to the optimum results in each examined case was determined.

(c) Activation functions of neurons: Two different types of activation functions for neurons of the hidden layers as well as the output layer were used: the sigmoid function (logistic–"logsig" or "log" function) and the hyperbolic tangent ("tansig" or "tan" function) function (see e.g. Haykin 2009). The choice of using two activation functions (instead of using a single one) was made in order to investigate the optimum efficiency of networks.

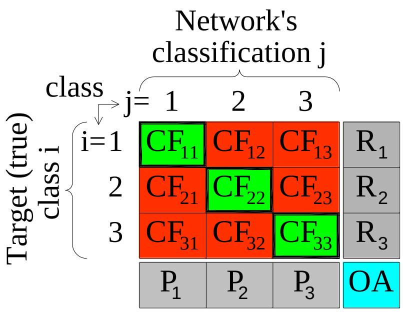

CF_{ij} = the number of the input vectors whose true class is i and were classified by the ANN to class j

$$R_i\,(\text{Recall}) = CF_{ii} \,/ \sum_{j=1}^{3} CF_{ij}$$

(the percentage of input vectors of true class i which were correctly classified by the ANN to class i)

$$P_j\,(\text{Precision}) = CF_{jj} \,/ \sum_{i=1}^{3} CF_{ij}$$

(the percentage of input vectors which were classified by the ANN into class j, whose true class is j)

$$\text{OA (Overall Accuracy)} = \sum_{i=1}^{3} CF_{ii} \,/\, N$$

(the percentage of input vectors that correctly classified by the ANN)

(N=total number of input and target vectors)

Fig. 4 General form of a confusion matrix for a three-class problem

(d) Performance evaluation parameters: The performance evaluation parameters are indices which are used for the assessment of networks' prediction abilities. In the case of solution of a pattern recognition problem the most useful tools for the evaluation of networks are the Confusion Matrices - CM (see e.g. Theodoridis and Koutroumbas 2008). The general form of a CM (for a three-class problem) is presented in Fig. 4.

On the basis of CMs three types of metrics for networks' prediction accuracy are defined, namely the "Recall" index, the "Precision" index and the "Overall Accuracy" index (Fig. 4). In the present study, the "Overall Accuracy" or (OA) index was mainly used. However, for the evaluation of the several configurations of the networks which were examined the corresponding CMs are also presented and evaluated.

(e) Normalization functions for the input and target vectors' elements: The utilization of functions which normalize the values of the elements of input vectors before these vectors are introduced in the networks is considered as necessary in order to optimize the training (e.g. Rafiq and Bugmann 2001). The same transformation is also required for the elements of the target vectors. A function, through which the elements of input and the target vectors of the data set attain values in the range [-1,1], was selected in the present study (Matlab 2015).

(f) Partition of the data-set: The partition of the data-set in three sub-sets: the training, the validation and the testing sub-set is recommended in order to ensure good generalization of networks and to avoid the overfitting (e.g. Hagan *et al*. 1996). In the present study, the partition of the data-set in training, validation and testing sub-sets was done using the ratio 70%/15%/15% respectively. Furthermore, the partition of the data-set in the three sub-sets was made using the ratio 50%/25%/25%. The training and target vectors, which consist of the three sub-sets, were chosen in any case randomly (Matlab 2015).

Finally, as regards the training algorithms, two algorithms were adopted: The Resilient Backpropagation algorithm ("RP" algorithm, Riedmiller and Braun 1993) and the Scaled Conjugate Gradient algorithm ("SCG" algorithm, Moller 1993). It must be also noted that, for the configuration and the training of networks, the neural network tool box in Matlab (2015) was used.

4. Comparative assessment of results

In the present section the results of the parametric investigation that has conducted in order to find the optimum combination of the parameters which determine the ANNs' configuration will be presented. Furthermore, it will be presented the results of the investigation for the reliability level of the predictions that the optimum configured ANNs can extract in cases for which they have not been trained (generalization ability). The parameters that have been investigated were presented in previous section. It must be noticed that the parametric analyses were conducted separately for the case of the 3 and the 5 damage classes (Table 2). Moreover, note that all results which concern the investigation of the optimum configuration of networks are based on the testing sub-set. This choice was made having in mind the fact that this sub-set consists of samples that are not used for the calculation of the weights of neurons' synapses but only for the test of the networks' generalization ability level during their training. Thus, the networks that accomplish the optimum performance for the samples of the testing sub-set are expected to have better generalization abilities.

4.1 Results of the Parametric Investigation for the Optimum Configuration of Networks

4.1.1 Investigation in the case of the consideration of 5 damage classes

Fig. 5 illustrates the maximum values of percentages of correct classifications which are extracted by networks (OA index, Fig. 4). The results are presented separately for each building type of the five ones that were considered in the present study (see Appendix A), as well as for all of them as a whole. As mentioned above, for each one of the five types of R/C buildings different networks were configured. Thus, the investigation for the ANNs' optimum parameters' combination was conducted separately for each one of buildings' types, leading to different optimum networks. Consequentially, the values of the OA index presented in Fig. 5 have resulted from different networks. It must also be noticed that the values of the OA index that correspond to the five buildings as a whole are the average values of the corresponding OA index values of each building.

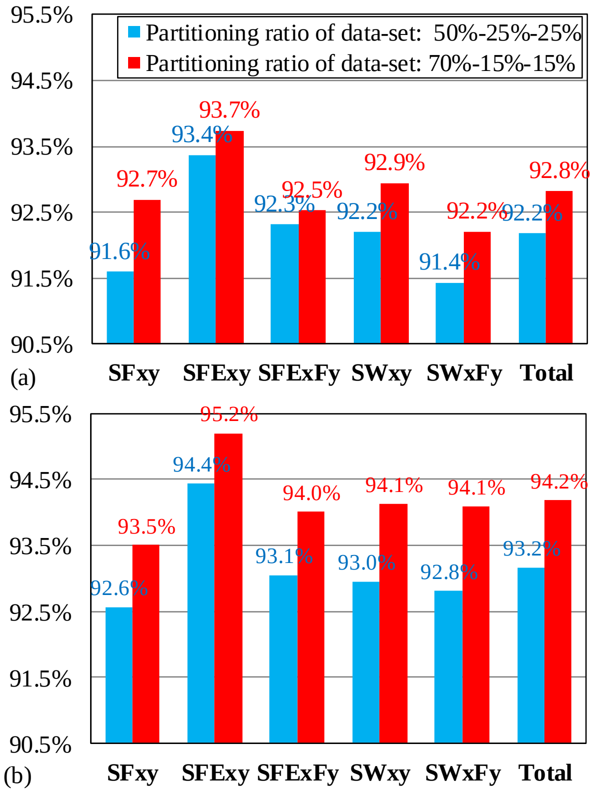

Fig. 5 Optimum (maximum) values of OA index in the case of 5 damage classes: (a) Networks with 1 hidden layer, (b) Networks with 2 hidden layers

From the study of Fig. 5 the following main conclusions can be drawn:

- All the optimum configured networks extract very sufficient percentages of correct classifications, since the OA index exceeds the value of 91% in all the cases.
- The addition of the second hidden layer leads to increase of the values of OA index. However, from the comparative study of the corresponding values of the diagrams presented in Figs. 5(a) and 5(b) it can be deduced that this increase cannot be considered as very significant. Anywise, the values of OA index which result from the networks with one hidden layer are especially high, since for all the buildings' types they exceed 91% (Fig. 5(a)).
- The partition of the total data set to three sub-sets using the ratio 70%/15%/15% leads in all cases to a more effective training of networks. However, in general, the optimization of the results that is due to this partition ratio is not especially important compared to the ratio 50%/25%/25%, since the respective increase of the values of the OA index is not greater than 2% in any case.
- The influence of the buildings' type on the maximum value of the OA index that can be achieved is, in general, greater in the case of networks with one hidden layer. As it can be seen in Fig. 5(a), the value of the OA index fluctuates in the range of 91.4% and 93.4% in case of networks with one hidden layer when the total data set's partition ratio is 50%/25%/25% (the corresponding range is 92.2%-93.7% when the partition ratio is 70%/15%/15%). Namely, in case of networks with one hidden layer the difference between the maximum and the minimum value of the OA index is about 2.0%. Correspondingly, in case of networks with two hidden layers, with the exception of the SFExy type, the respective differences between the maximum and the minimum value of the OA index are about 0.5% (Fig. 5(b)).

Table 3 Optimum configuration parameters of networks with 1 hidden layer in case of 5 damage classes

	Partitioning ratio of the total data set					
	50%/25%/25%			70%/15%/15%		
	Training algorithm	Activation function of neurons in the hidden / output layer	Neurons in the hidden layer	Training algorithm	Activation function of neurons in the hidden / output layer	Neurons in the hidden layer
SFxy	SCG	tan / tan	44	SCG	tan / tan	36
SFExy	SCG	log / tan	34	RP	log / tan	46
SFExFy	SCG	log / tan	46	SCG	log / tan	46
SWxy	RP	tan / tan	48	RP	log / tan	42
SWxFy	SCG	log / tan	54	RP	log / tan	54

Table 4 Optimum configuration parameters of networks with 2 hidden layers in case of 5 damage classes

	Partitioning ratio of the total data set					
	50%/25%/25%			70%/15%/15%		
	Training algorithm	Activation function of neurons in two hidden / output layer	Neurons in the two hidden layers	Training algorithm	Activation function of neurons in two hidden / output layer	Neurons in the two hidden layers
SFxy	RP	tan / tan / tan	58 / 32	SCG	tan / log /tan	48 / 26
SFExy	RP	tan / log /tan	32 / 44	RP	log / tan / tan	56 / 50
SFExFy	SCG	tan / log /tan	56 / 54	SCG	tan / tan / tan	48 / 58
SWxy	RP	log / log/ tan	60 / 24	SCG	tan / tan / tan	22 / 52
SWxFy	SCG	tan / tan / tan	36 / 58	RP	tan / tan / tan	56 / 56

Classification of network

Target class	1	2	3	4	5	R
1	**399**	9	0	0	0	97.8%
2	12	**264**	7	1	0	93.0%
3	0	19	**442**	21	4	90.9%
4	0	0	5	**111**	12	86.7%
5	0	0	0	6	**166**	96.5%
P	97%	90.4%	97.4%	79.9%	91.2%	***93.5%***

Building SFxy

Classification of network

Target class	1	2	3	4	5	R
1	**409**	2	1	0	0	99%
2	11	**229**	14	1	0	89.8%
3	0	10	**411**	14	2	94.1%
4	0	0	11	**154**	4	91.1%
5	0	0	1	1	**226**	99.1%
P	97.4%	95.0%	93.8%	90.6%	97.4%	***95.2%***

Building SFExy

Classification of network

Target class	1	2	3	4	5	R
1	**277**	11	1	0	0	95.8%
2	4	**147**	7	1	1	91.9%
3	0	8	**333**	13	3	93.3%
4	0	0	15	**214**	8	90.3%
5	0	0	1	0	**174**	99.4%
P	98.6%	88.6%	93.3%	93.9%	93.5%	***94.0%***

Building SFExFy

Classification of network

Target class	1	2	3	4	5	R
1	**404**	9	0	0	0	97.8%
2	9	**259**	15	1	1	90.9%
3	0	10	**416**	12	0	95.0%
4	0	0	5	**139**	11	89.7%
5	0	0	0	11	**129**	92.1%
P	98%	93.2%	95.4%	85.3%	91.5%	***94.1%***

Building SWxy

Classification of network

Target class	1	2	3	4	5	R
1	**299**	6	2	0	0	97.4%
2	8	**189**	5	0	0	93.6%
3	0	8	**360**	14	3	93.5%
4	0	0	15	**137**	3	88.4%
5	0	0	0	8	**162**	95.3%
P	97.4%	93.1%	94.2%	86.2%	96.4%	***94.1%***

Building SWxFy

Classification of network

Target class	1	2	3	4	5	R
1	**1788**	37	4	0	0	97.8%
2	44	**1088**	48	4	2	91.7%
3	0	55	**1962**	74	12	93.3%
4	0	0	51	**755**	38	89.5%
5	0	0	2	26	**857**	96.8%
P	98%	92.2%	94.9%	87.9%	94.3%	***94.2%***

All buildings

Fig. 6 CMs of the classifications exported by the optimum configured ANNs in case of 5 damage classes

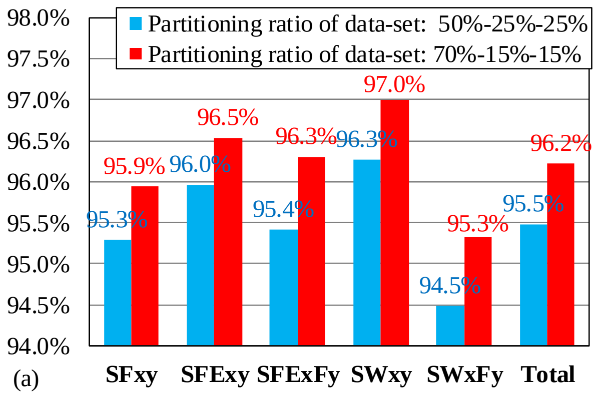

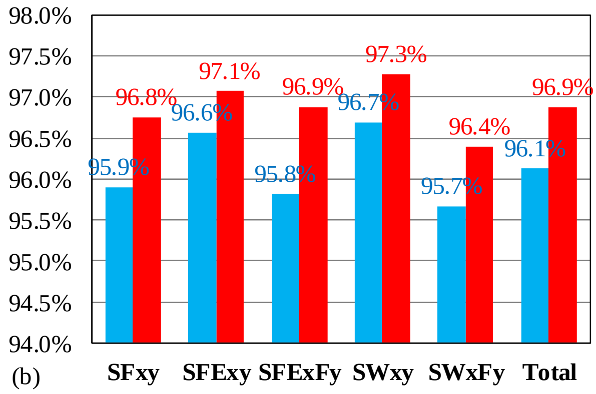

Fig. 7 Optimum (maximum) values of OA index in the case of 3 damage classes: (a) Networks with 1 hidden layer, (b) Networks with 2 hidden layers

Tables 3 and 4 present the parameters that configure the optimum networks (namely, the networks that extract the values of the OA index given in Fig. 5).

From the study of Tables 3 and 4 the following main conclusions can be drawn:

- The buildings' type and, consequently, the total data set, influences the whole set of the parameters that configure the optimum networks. The same conclusion is valid for the partition ratio used to divide the total data set in three sub-sets.
- The number of neurons in hidden layers differentiates in a random way in any case. This fact documents the well-known rule that there is no certain direct method for the determination of neurons' optimum number but the parametric investigation.
- No certain trend can be found with respect to the more efficient training algorithm between RP and SCG.
- Different optimum combinations appear for the activation functions in the hidden layer(s) and the output layer. However, all these combinations have as a common characteristic that for the output layer the optimum choice is the function tan (tansig).

Fig. 6 illustrates the confusion matrices (CMs) that result from the classifications which are extracted by the most efficient of the optimum networks given in the Tables 3 and 4. It must be noticed that, based on the results presented in Fig. 5 and in Tables 3 and 4, these CMs arise from networks with two hidden layers which were trained using the ratio 70%/15%/15% for the partition of the total data set in the three sub-sets (see Fig. 5(b)). From the study of Fig. 6 it can be seen that, except for the especially large percentage of correct classifications in the corresponding damage classes, it is also evident that the incorrect classifications correspond to classifications of the buildings to damage classes which are adjacent to the correct ones.

Table 5 Optimum configuration parameters of networks with 1 hidden layer in case of 3 damage classes

	Partitioning ratio of the total data set					
	50%/25%/25%			70%/15%/15%		
	Training algorithm	Activation function of neurons in the hidden / output layer	Neurons in the hidden layer	Training algorithm	Activation function of neurons in the hidden / output layer	Neurons in the hidden layer
SFxy	SCG	tan / tan	48	RP	tan / tan	58
SFExy	RP	tan / tan	56	RP	log / tan	48
SFExFy	SCG	tan / tan	34	RP	tan / tan	52
SWxy	RP	log / tan	44	RP	tan / tan	50
SWxFy	SCG	tan / tan	58	SCG	log / tan	48

Table 6 Optimum configuration parameters of networks with 2 hidden layers in case of 3 damage classes

	Partitioning ratio of the total data set					
	50%/25%/25%			70%/15%/15%		
	Training algorithm	Activation function of neurons in two hidden / output layer	Neurons in the two hidden layers	Training algorithm	Activation function of neurons in two hidden / output layer	Neurons in the two hidden layers
SFxy	SCG	tan / log /tan	44 / 34	RP	tan / log /tan	60 / 32
SFExy	RP	tan / tan / tan	22 / 38	RP	tan / tan / tan	36 / 26
SFExFy	RP	tan / tan / tan	54 / 54	RP	tan / tan / tan	50 / 54
SWxy	SCG	log / log /tan	60 / 48	RP	tan / log /tan	40 / 30
SWxFy	RP	tan / tan / tan	44 / 46	RP	tan / tan / tan	56 / 38

Classification of network

Target class	1	2	3	R
1	**636**	7	2	98.6%
2	11	**468**	25	92.9%
3	0	3	**326**	99.1%
P	98%	97.9%	92.4%	***96.8%***

Building SFxy

Classification of network

Target class	1	2	3	R
1	**614**	8	0	98.7%
2	14	**431**	15	93.7%
3	0	7	**412**	98.3%
P	97.8%	96.6%	96.5%	***97.1%***

Building SEFxy

Classification of network

Target class	1	2	3	R
1	**460**	5	0	98.9%
2	4	**318**	21	92.7%
3	0	8	**402**	98.0%
P	99.1%	96.1%	95.0%	***96.9%***

Building SFExFy

Classification of network

Target class	1	2	3	R
1	**668**	11	0	98.4%
2	12	**410**	9	95.1%
3	0	7	**314**	97.8%
P	98%	95.8%	97.2%	***97.3%***

Building SWxy

Classification of network

Target class	1	2	3	R
1	**472**	7	1	98.3%
2	8	**384**	16	94.1%
3	0	12	**319**	96.4%
P	98.3%	95.3%	94.9%	***96.4%***

Building SWxFy

Classification of network

Target class	1	2	3	R
1	**2850**	38	3	98.6%
2	49	**2011**	86	93.7%
3	0	37	**1773**	98.0%
P	98%	96.4%	95.2%	***96.9%***

All buildings

Fig. 8 CMs of the classifications exported by the optimum configured ANNs in case of 3 damage classes

This means that even if an incorrect classification arises, the error will be not especially important (see e.g. Morfidis and Kostinakis 2017, 2018).

4.1.2 Investigation in the case of the consideration of 3 damage classes

Fig. 7 illustrates the maximum values of the percentage of correct classifications that are extracted by the optimum configured networks (OA index, Fig. 4). The results are presented separately for each building type of the five ones that were considered, as well as for all of them as a whole.

The results of Fig. 7 are similar with those that were extracted for the case of considering 5 damage classes (Fig. 5). The only exception is the fact that the influence of the buildings' type on the maximum value of the OA that can be achieved is, in general, larger when 3 damage levels are considered. Finally, it must be noticed that from the combined study of Figs. 5 and 7 it can be seen that when 3 damage classes are taken into consideration the optimum configured networks achieve larger percentages of correct predictions. This conclusion is generally expected, since the consideration of 3 damage levels makes the problem less complicated than in case of 5 damage classes, thus making the training algorithms more efficient.

Tables 5 and 6 present the parameters that configure the optimum networks (namely the networks that extract the values of OA index given in Fig. 7). The conclusions which are drawn from the study of these tables are corresponding to the ones that were extracted from the study of Tables 3 and 4, which concern the case of 5 damage classes.

In Fig. 8 the confusion matrices (CMs) that result from the classification of the most efficient of the optimum networks given in Tables 5 and 6 are presented. As in the case of 5 seismic damage classes, it must be noticed that, based on the results illustrated in Fig. 7 and in Tables 5 and 6, these CMs arise from networks with two hidden layers which were trained using the ratio 70%/15%/15% for the partition of the total data set in the three sub-sets (see Figs. 5(b), 7(b)). Also, as in the case of 5 seismic damage classes, from the study of Fig. 8 it can be seen that the vast majority of the examined samples is classified by the ANNs in the

Table 7 Details and names of the optimum networks in case of 5 damage classes

	Training algorithm	Activation function of neurons in two hidden / output layer	Neurons in the two hidden layers	Partitioning ratio of the total data set	Name
SFxy	SCG	tan / log /tan	48 / 26	70%/15%/15%	N2-TLT-48/26-SCG
SFExy	RP	log / tan / tan	56 / 50	70%/15%/15%	N2-LTT-56/50-RP
SFExFy	SCG	tan / tan / tan	48 / 58	70%/15%/15%	N2-TTT-48/58-SCG
SWxy	SCG	tan / tan / tan	22 / 52	70%/15%/15%	N2-TTT-22/52-SCG
SWxFy	RP	tan / tan / tan	56 / 56	70%/15%/15%	N2-TTT-56/56-RP

Table 8 Details and names of the optimum networks in case of 3 damage classes

	Training algorithm	Activation function of neurons in two hidden / output layer	Neurons in the two hidden layers	Partitioning ratio of the total data set	Name
SFxy	RP	tan / log /tan	60 / 32	70%/15%/15%	N2-TLT-60/32-RP
SFExy	RP	tan / tan / tan	36 / 26	70%/15%/15%	N2-TTT-36/26-RP
SFExFy	RP	tan / tan / tan	50 / 54	70%/15%/15%	N2-TTT-50/54-RP
SWxy	RP	tan / log /tan	40 / 30	70%/15%/15%	N2-TLT-40/30-RP
SWxFy	RP	tan / tan / tan	56 / 38	70%/15%/15%	N2-TTT-56/38-RP

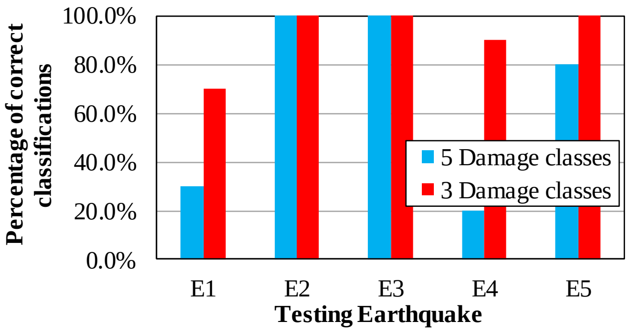

Fig. 9 Results of the generalization ability test of the optimum configured and trained networks

correct seismic damage class. Moreover, the samples that are classified in damage classes which are not adjacent to the correct ones are very little.

4.2 Results of the Generalization Ability Testing of the Optimum Configured Networks

In this subsection the results of the generalization tests of the optimum configured and trained networks will be presented. These networks have been resulted from the parametric investigation that was presented in previous subsection. Based on the results of this investigation (Figs. 5, 7 and Tables 3, 4, 5, 6), the optimum configured networks that will be examined have two hidden levels and for their training the partition of the total data set in the three sub-sets was made using the ratio 70%/15%/15% (training sub-set: 70%, validation sub-set: 15%, testing sub-set: 15%). Tables 7 and 8 present the parameters along with the names that were given to the optimum ANNs which were used for the generalization ability tests.

For the generalization ability tests of the optimum configured networks given in Tables 7 and 8, 5 seismic motions different from the 65 ones that were used for their training were selected. Additionally, for each one of the 5 examined buildings' types, 2 different masonry infills' distributions were chosen, which were also different from the ones considered for the formulation of the total training data set. Thus, for each one of the 5 buildings' types, 10(=5x2) testing samples were formed, namely buildings with infills' distributions unknown to networks, which were analyzed using 5 also unknown to them seismic motions. For these cases the value of MIDR was extracted from the optimum ANNs given in Tables 7 and 8. Furthermore, the MIDR index was calculated for the same cases using NTHA.

Fig. 9 presents for each one of the 5 testing earthquakes the percentage of the cases for which the optimum configured networks extracted correct classifications.

From the study of the Fig. 9 it can be clearly seen that the generalization ability of the networks is much larger when 3 seismic damage classes are taken into account. More specifically, in this case the percentages of correct predictions of the optimum configured networks are larger than 70% for all the testing earthquakes. For the testing earthquakes E2, E3 καιE5 the best configured networks achieve correct predictions for the whole set of examined samples. On the contrary, in the case of considering 5 damage classes, and despite the fact that for the testing earthquakes E2, E3 καιE5 the percentages of the correct classifications are especially high, for the testing earthquakes E1 καιE4 the corresponding percentages are rather low (smaller than 30%) and, thus, not acceptable.

5. Conclusions

The objective of the present paper is to examine the ability of ANNs to adequately predict the seismic damage of 3D R/C buildings with various distributions of masonry infills. The application of ANNs for the solution of this problem adds an important computational tool to the procedure of effective seismic design of R/C buildings, since it gives the ability of direct estimation, at the level of initial design, of the increase of the seismic vulnerability that can be caused by a chosen masonry infills' distribution. To accomplish this purpose an extensive parametric study is carried out. More specifically, five 3-dimensional 5-storey R/C buildings with symmetric plan view and different structural systems are studied. For each building a large number of different masonry infills' distributions is considered. The infilled buildings are analyzed by means of Nonlinear Time History Analysis (NTHA) for 65 bidirectional strong motions and four different incident angles (θ=0°, 90°, 180° and 270°). For the evaluation of the seismic damage of each building the maximum interstorey drift ratio (MIDR) is computed. Then, ANNs are utilized in order to effectively predict the seismic damage.

The problem was formulated and solved as a pattern recognition problem. Thus, the extracted results are the classification of the examined buildings in one of the predefined damage classes, which are defined on the basis of certain values of the MIDR damage index. In the context of the present investigation five, as well as three seismic damage classes are considered. The type of the networks that are used is “Multilayer Feedforward Perceptron” with one or two hidden neurons' layers, whereas an investigation for the optimum combination of activation functions in the hidden and the output neurons' layers is conducted. Moreover, the optimum number of neurons in the hidden layers is also investigated. As input parameters of the networks 14 well-known from the literature seismic parameters, as well as 4 parameters that describe the percentage and the distribution of the masonry infills in a building are used. Different training data sets for each one of the examined buildings' types are generated. From the parametric investigation of the optimum combination of the ANNs' configuration parameters optimum networks for each one of these types are resulted. These optimum ANNs are used for the generalization tests, namely for the tests of the reliability of the predictions that are extracted by the networks in cases for which they have not been trained. The generalization tests that are conducted led to the main conclusion that the networks with two hidden layers are able to extract in real time reliable predictions for the seismic vulnerability of masonry infilled R/C buildings with certain infills' distribution, mainly in the case of consideration of three seismic damage classes (Slight-Moderate-Heavy). Thus, a civil engineer who uses properly trained ANNs at the stage of a R/C building's design, will be capable of knowing in a very short time and with a high degree of reliability if a chosen masonry infills' distribution is possible to lead to moderate or severe seismic damages and, so, he can decide if he (she) will change or improve it. It must be noted that the structural models investigated in the present study consist of 3-D buildings with typical simple plan-views and not of real reinforced concrete structures, since the aim of the study is to make a first approach at the investigation of the ANNs' ability to predict the seismic damage. This is the reason why simple buildings with certain ranges of structural characteristics are chosen. In order to generalize the abovementioned ANNs' ability in case of other buildings too, it is necessary to use a much bigger sample of training data sets than the one used here (which consists of 49,335 samples) and to take into consideration other structural parameters too, e.g. soil type, material properties, dimensions along axes x and y etc.

Acknowledgment

This study was financially supported by A.U.Th. Research Committee (Fellowships of Excellence for Postgraduate Studies 2015).

References

Adeli, H. (2001), “Neural networks in civil engineering: 1989-2001”, *Comput Aid Civ Infrastruct Eng*, **16**, 126–42. https://doi.org/10.1111/0885-9507.00219.

Akbas, B., Shen, J. and Sabol, T.A. (2011), “Estimation of seismic-induced demands on column splices with a neural network model”, *Appl. Soft Comput.*, **11**(8), 4820-4829.

Anagnos, T., Rojahn, C. and Kiremidjian, A.S. (1995), “NCEER-ATC joint study on fragility of buildings”, Technical Report NCEER 95-0003; State University of New York at Buffalo, National Center for Earthquake Engineering Research, USA.

Asht, S. and Dass, R. (2012), “Pattern Recognition Techniques: A Review”, *J. Comput. Sci. Telecommunications*, **3**(8), 25-29.

ATC-63, FEMA P695 (2008), *Quantification of Building Seismic Performance Factors*, FEMA, D.C. Washington, USA.

ATC (1985), “Earthquake damage evaluation data for California”, ATC-13 Report; Applied Technology Council, Redwood City, CA, USA.

Bertero, V.V. and Brokken, S. (1983), “Infills in seismic resistant buildings”, *J. Struct. Eng. ASCE*, **109**(6), 1337-1361.

Carr A. (2004), *Ruaumoko – A Program for Inelastic Time-History Analysis*, Department of Civil Engineering, University of Canterbury, New Zealand.

Crisafulli, F.J. (1997), “Seismic behaviour of reinforced concrete structures with masonry infills”, Ph.D. Dissertation, University of Canterbury, Christchurch, New Zealand.

EERI (2000), “1999 Kocaeli, Turkey earthquake reconnaissance report”, *Earthq. Spectra*, **16**(S1), 237-379.

EN1998-1 (2003), “Design of structures for earthquake resistance - Part 1: General rules, seismic actions and rules for buildings”, European Committee for Standardization, Brussels, Belgium.

EN1992-1-1 (2003), “Design of Concrete Structures, Part 1-1: General rules and rules for buildings”, European Committee for Standardization, Brussels, Belgium.

EN1996-1-1 (2005), “Design of masonry structures - Part 1-1: General rules for reinforced and unreinforced masonry structures, European Committee for Standardization, Brussels, Belgium.

European Strong-Motion Database (2003), Internet Site for European Strong-Motion Data, European Strong-Motion Database, http://www.isesd.hi.is/ESD_Local/frameset.htm.

Fausett, L. (1994), *Fundamentals of Neural Networks: Architectures, Algorithms and Applications*, Pearson, London, United Kingdom.

Fiore A., Porco F., Raffaele D. and Uva G. (2012), “About the influence of the infill panel over the collapse mechanisms actived under pushover analyses: Two case studies”, *Soil Dynam. Earthq. Eng.*, **39**, 11–22. https://doi.org/10.1016/j.soildyn.2012.02.004.

Fontara, I-K.M., Kostinakis, K.G., Manoukas, G.E., Athanatopoulou, A.M. (2015), “Parameters affecting the seismic response of buildings under bi-directional excitation”, *Struct. Eng. Mech.*, **53**(5), 957-979. http://dx.doi.org/10.12989/sem.2015.53.5.957.

Gunturi, S.K.V., Shah, HC. (1992), “Building specific damage estimation", *Proceedings of 10th World Conference on Earthquake Engineering*, Balkema, Madrid-Rotterdam, Spain. 6001-6006.

Hagan, M.T., Demuth, H.B. and Beale, M.H. (1996), *Neural Network Design*, PWS Publishing, Boston.

Haykin, S. (2009), *Neural Networks and Learning Machines*, 3rd ed. Prentice Hall, Pearson, USA.

IBC-2018 (2018), International Code Council (ICC).

Imbsen Software Systems (2006), *XTRACT: Version 3.0.5. Cross-Sectional Structural Analysis of Components*, Sacramento, CA, USA.

Jegadesh, S.J.S. and Jayalekshmi, S. (2015), "A review on artificial neural network concepts in structural engineering applications", *Int. J. Appl. Civ. Env. Eng.*, **1**(4), 6–11.

Kappos, A. and Penelis, G.G. (1997), *Earthquake Resistant Concrete Structures*, E & FN Spon., Taylor and Francis, USA.

Kappos, A.J., Panagopoulos, G, Panagiotopoulos, C., Penelis G., (2006), "A hybrid method for the vulnerability assessment of R/C and URM buildings", *Bull Earthq. Eng*, **4**(4), 391-413. https://doi.org/10.1007/s10518-006-9023-0.

Kostinakis, K., Vasileiadis, V. and Athanatopoulou, A. (2018), "Incremental dynamic analysis of R/C buildings with various ditributions of masonry infills", *Proceedings of 16th European Conference on Earthquake Engineering*, Thessaloniki, Greece, June.

Kostinakis, K., Athanatopoulou, A. and Avramidis, I. (2013), "Evaluation of inelastic response of 3D single-story R/C frames under bi-directional excitation using different orientation schemes", *Bull Earthq Eng*, **11**, 637-661. https://doi.org/10.1007/s10518-012-9392-5.

Kostinakis, K., Morfidis, K., Xenidis, H. (2015), "Damage response of multistorey r/c buildings with different structural systems subjected to seismic motion of arbitrary orientation", *Earthq. Eng. Struct. Dynam.*, **44**, 1919-1937. https://doi.org/10.1002/eqe.2561.

Kostinakis, K., Manoukas, G. and Athanatopoulou, A. (2018), "Influence of Seismic Incident Angle on Response of Symmetric in Plan Buildings", *KSCE J. Civil Eng.*, **22**(2), 725-735. https://doi.org/10.1007/s12205-017-1279-1.

Kramer, S.L. (1996), *Geotechnical Earthquake Engineering*, Prentice-Hall, USA.

Lagaros, N.D. and Papadrakakis, M. (2012), "Neural network based prediction schemes of the non-linear seismic response of 3D buildings", *Adv. Eng. Software*, **44**(1), 92-115. https://doi.org/10.1016/j.advengsoft.2011.05.033.

Lautour, O.R. and Omenzetter, P. (2009), "Prediction of seismic-induced structural damage using artificial neural networks", *Eng Struct*, **31**, 600–606. https://doi.org/10.1016/j.engstruct.2008.11.010.

Manfredi, G., Ricci, P. and Verderame G.M. (2012), "Influence of Infill Panels and their Distribution on Seismic Behavior of Existing Reinforced Concrete Buildings", *The Open Construct. Building Technol. J.*, **6**(Suppl 1-M15), 236-253. http://dx.doi.org/10.2174/1874836801206010236.

Masi, A., Vona, M. and Mucciarelli, M. (2011), "Selection of Natural and Synthetic Accelerograms for Seismic Vulnerability Studies on Reinforced Concrete Frames", *J Struct Eng*, **137**, 367-378.

Matlab (2015), *Neural Networks Toolbox User Guide*, Mathworks, MA, USA.

Moller, M.F. (1993), "A scaled conjugate gradient algorithm for fast supervised learning", *Neural Netw*, **6**, 525–33. https://doi.org/10.1016/S0893-6080(05)80056-5.

Mondal, G. and Tesfamariam, S. (2014), "Effects of vertical irregularity and thickness of unreinforced masonry infill on the robustness of RC framed buildings", *Earthquake Engineering and Structural Dynamics*, **43**, 205-223. https://doi.org/10.1002/eqe.2338.

Morfidis, K.E. and Kostinakis, K.G. (2017), "Approach to prediction of R/C buildings' seismic damage as pattern recognition problem using artificial neural networks", *Proceedings of 4th Conference in Computational Methods in Structural Dynamics and Earthquake Engineering (COMPDYN2017)*, Rhodes Island, Greece, June.

Morfidis, K. and Kostinakis, K. (2018), "Approaches to the rapid seismic damage prediction of r/c buildings using artificial neural networks", *Engineering Structures*, **165**, 120-141. https://doi.org/10.1016/j.engstruct.2018.03.028.

Morfidis, K. and Kostinakis K. (2017), "Seismic parameters' combinations for the optimum prediction of the damage state of R/C buildings using neural networks", *Adv. Eng. Software*, **106**, 1-16. https://doi.org/10.1016/j.advengsoft.2017.01.001.

Morfidis, K. and Kostinakis, K. (2019), "Comparative evaluation of MFP and RBF neural networks' ability for instant estimation of r/c buildings' seismic damage level", *Eng. Struct.*, **197**, paper: 109436.

Naeim, F. (2001), *The Seismic Design Handbook*, 1st Ed., Kluwer Academic, Boston, MA, USA.

Nguyen, V. T. and Kim, D. (2013), "Influence of incident angles of earthquakes on inelastic responses of asymmetric-plan structures", *Struct. Eng. Mech.*, **45**(3), 373-389. https://doi.org/10.12989/sem.2013.45.3.373.

Otani, A. (1974), "Inelastic Analysis of RC frame structures", *J Struct Div (ASCE)*, **100**(7), 1433-1449.

Pacific Earthquake Engineering Research Centre (PEER), (2003), "Strong Motion Database". https://ngawest2.berkeley.edu/.

Paulay, T. and Priestley, M.J.N. (1992), *Seismic Design of Reinforced Concrete and Masonry Buildings*, John Wiley & Sons, Inc., NJ, USA.

Rafiq, M.Y., Bugmann, G. and Easterbrook, D.J. (2001), "Neural network design for engineering applications" *Comput. Struct.*, **79**, 1541–1552. https://doi.org/10.1016/S0045-7949(01)00039-6.

Ricci, P., De Luca, F. and Verderame, G.M. (2010), "6th April 2009 L' Aquila earthquake, Italy: reinforced concrete building performance", *Bullet. Earthq. Eng.*, **9**(1), 285-305. https://doi.org/10.1007/s10518-010-9204-8.

Ricci, P., De Ricci, M.T., Verderame, G.M. and Manfredi, G. (2013), "Influence of infill distribution and design typology on seismic performance of low-and mid-rise RC buildings", *Bulletin of Earthquake Engineering*, **11**, 1585-1616. https://doi.org/10.1007/s10518-013-9453-4.

Ricci, P., Verderame, G.M. and Manfredi, G. (2011), "Analytical investigation of elastic period of infilled RC MRF buildings", *Eng. Struct.*, **33**, 308-319. https://doi.org/10.1016/j.engstruct.2010.10.009.

Riedmiller, M., Braun, H. (1993), "A Direct Adaptive Method for Faster Backpropagation Learning: The RPROP Algorithm", *IEEE International Conference on Neural Networks, San Francisco, CA*, April-March. 586-591.

Rigato, A. and Medina, R. (2007), "Influence of angle of incidence on seismic demands for inelastic single-storey structures subjected to bi-directional ground motions", *Eng. Struct.*, **29**, 2593–2601. https://doi.org/10.1016/j.engstruct.2007.01.008.

Ripley, B.D. (1996), *Pattern Recognition and Neural Networks*, Cambridge University Press, United Kingdom.

Theodoridis, S., Koutroumbas, K. (2008), *Pattern Recognition*. 4th ed., Elsevier, The Netherlands.

Vafaei. M., Adnan, A., Yadollahi, M. (2011), "Seismic damage detection using pushover analysis", *Adv. Mater. Res.*, **255-260**, 2496-2499.

Vafaei, M., Adnan, A.B., Rahman, A.B.A. (2013), "Real-time seismic damage detection of concrete shear walls using artificial neural networks", *J. Earthq. Eng.*, **17**, 137–154. https://doi.org/10.1080/13632469.2012.713559.

Vafaei, M., Adnan, A., Rahman, A.B.A. (2014), “A neuro-wavelet technique for seismic damage identification of cantilever structures”, *Struct. Infrastruct. Eng.*, **10**(12), 1666-1684. https://doi.org/10.1080/15732479.2013.849746.

CC

APPENDIX A:
Design data of the 5 selected R/C buildings

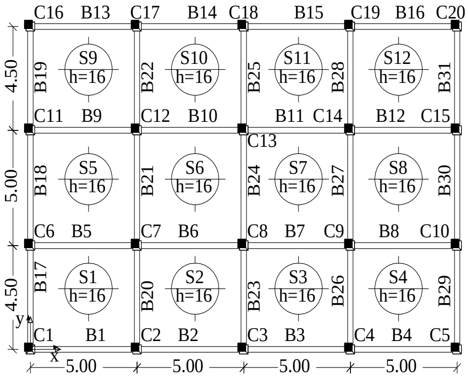

Storey	Beams	Columns
1st-2nd	25/65	45/45
3rd	25/60	40/40
4th	25/55	35/35
5th	20/45	35/35

n_{vx}	n_{vy}
0.0%	0.0%

Behavior factor: q=3.9

(a) Symmetric Frame System along both axes x and y (SFxy)

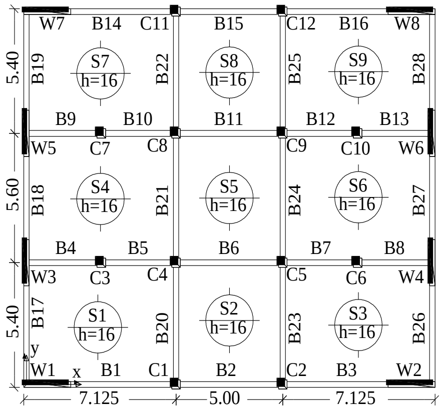

Storey	Beams	Columns	Walls
1st	25/55	C1,C2,C11,C12: 35/35 C3,C6,C7,C10: 30/30 C4,C5,C8,C9: 40/40	W1,W2, W7,W8 220/25
2nd-3rd	25/55 (B18,B27: 25/45)	35/35 (C3,C6,C7,C10: 30/30)	W3,W4, W5,W6 200/25
4th	25/50 (B18,B27: 25/45)	30/30	
5th	20/45		

n_{vx}	n_{vy}
77.0%	80.0%

Behavior factor: q=3.0

(c) Symmetric Wall System along both axes x, y (SWxy)

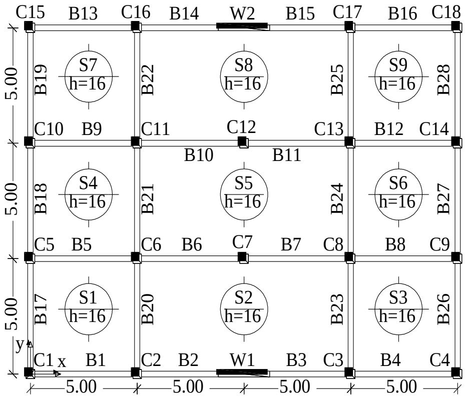

Data for SWxFy building

Storey	Beams	Columns	Walls
1st-2nd	25/55	40/40 (C7,C12:35/35)	240/25
3rd	25/50		
4th	25/50	35/35	
5th	20/45	30/30	

n_{vx}	n_{vy}
68.0%	0.0%

Behavior factor q=3.0

Data for SFExFy building

Storey	Beams	Columns	Walls
1st-2nd	25/55	40/40 (C7,C12:35/35)	130/25
3rd	25/50		
4th	25/50	35/35	
5th	20/45	30/30	

n_{vx}	n_{vy}
43.0%	0.0%

Behavior factor q=3.9

(b) Symmetric Wall System along axis x - Frame System along axis y (SWxFy) and Symmetric Frame-Equivalent System along axis x - Frame System along axis y (SFExFy)

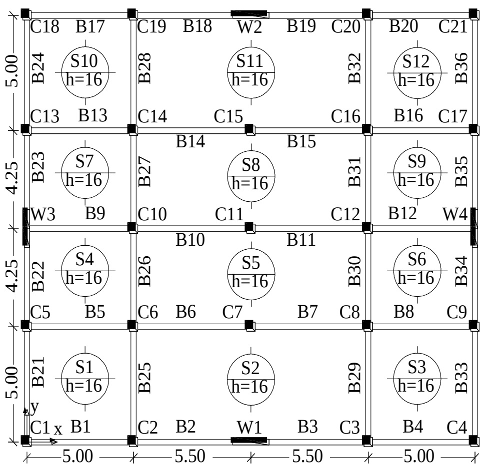

Storey	Beams	Columns	Walls
1st-2nd	25/55	40/40	W1,W2 170/25
3rd	25/50	35/35	
4th	25/50	35/35	W3,W4 165/25
5th	20/45	30/30	

n_{vx}	n_{vy}
46.0%	50.0%

Behavior factor: q=3.9

(d) Symmetric Frame-Equivalent System along axes x and y (SFExy)

Fig. A.1. Plan view and dimensions of the R/C members' cross-sections of the 5 selected r/c buildings

Table A.1 Common design data for all buildings

Storeys' heights H_i	Ductility class	Concrete	Steel	Slab loads	Masonry loads	Design spectrum (EN1998-1)
3.2m	Medium (DCM)	*C20/25* $E_c=3\cdot10^7$kN/m^2 ν=0.2 w=25kN/m^3	*S500B* $E_s=2\cdot10^8$kN/m^2 ν=0.3 w=78.5kN/m^3	*Dead*: G=1.0kN/m^2 *Live*: Q=2.0kN/m^2	*Perimetric beams*: 3.6kN/m^2 *Internal beams*: 2.1kN/m^2	*Reference PGA*: a_{gR}=0.24g *Importance class*: II → γ_I=1 *Ground type*: C